Electrocardiogram-gated 16-multidetector computed tomographic angiography of the coronary arteries in dogs

Auriemma, E ; Armienti, F ; Morabito, S ; Specchi, S ; Rondelli, V ; Domenech, O ; Guglielmini, C ; Lacava, G ; Zini, Eric ; Khouri, T

Abstract: The aims of this study were to assess if ECG-gated 16-multidetector CT (MDCT) provides sufficient temporal and spatial resolution to evaluate canine coronary arteries and provide a detailed description of their anatomy. A total of 24 dogs were included. Images were reviewed to assess: (1) coronary artery opacification and dominance; (2) choice of optimal R-R ECG reconstruction interval for both left coronary artery (LCA) and right coronary artery (RCA); (3) branching patterns of the left main coronary artery (LMCA); and (4) diameter and length of the LCA and RCA and classification of their branches by adapting a previously described segmental coding system. The degree of opacification of the coronary arteries was subjectively judged as excellent or good in five and 19 dogs, respectively. All hearts showed a left coronary dominance. The best R-R reconstruction interval for both LCA and RCA arteries was 75 per cent. Seven different subtypes of LMCA branching patterns were noted. The and were divided into three angiographic segments, and the and the RCA in two and three segments, respectively. ECG-gated 16-MDCT coronary angiography provides adequate resolution to assist the basic anatomy of the main coronary artery branches.

DOI: https://doi.org/10.1136/vr.104711

ECG-GATED 16-MULTIDETECTOR COMPUTED TOMOGRAPHIC ANGIOGRAPHY OF THE CORONARY ARTERIES IN DOGS

Edoardo Auriemma, DVM, ECVDI [1], Felice Armienti, DM [2], Simona Morabito, DVM [1,3], Giuseppe Lacava, DVM, ECVDI[1], Swan Specchi, DVM, PhD, DÈS, DACVR [1], Vincenzo Rondelli, DVM, PhD [1], Oriol Domenech, DVM, MSc, Dipl. ECVIM-CA (Cardiology)[1], Carlo Guglielmini, DVM, PhD [4], Eric Zini, DVM, PhD, PD, DECVIM-CA (Internal Medicine) [4,5], Toufic Khouri, DM [2]

[1] *Istituto Veterinario di Novara, Novara, Italy*
[2] *Diagnostic Imaging Department, Policlinico di Monza Hospital, Monza, Italy*
[3] *Department of Veterinary Science, University of Messina, Polo Universitario Annunziata 98168 Messina, Italy.*
[4] *Department of Animal Medicine, Production & Health, University of Padua, Padua, Italy*
[5] *Clinic for Small Animal Internal Medicine, Vetsuisse Faculty, Zurich, Switzerland.*

Abstract

The aims of the study were to assess if electrocardiogram-gated 16-multidetector computed tomography (MDCT) provides enough temporal and spatial resolution in order to evaluate canine coronary arteries and to provide detailed description of their anatomy.

A total of 24 dogs were included. Images were reviewed to assess: 1) coronary artery opacification and dominance, 2) choice of optimal R-R electrocardiogram reconstruction interval for both left (LCA) and right (RCA) coronary arteries, 3) branching patterns of the left main coronary segment (LMCA), 4) diameter and length of the LCA and RCA and classification of their branches by adapting a previously described segmental coding system.

The degree of opacification of the coronary arteries was subjectively judged excellent or good in 5 and 19 dogs, respectively. All hearts showed a left coronary dominance. The best R-R reconstruction interval for both LCA and RCA arteries was 75% (15 dogs). Seven different sub-types of LMCA branching patterns were noted. The *rami circumflexus* and *septi-interventricularis paraconalis* were divided into 3 angiographic segments, the *ramus septi inter-ventricularis* and the RCA in 2 and 3 segments, respectively.

Electrocardiogram-gated 16-MDCT coronary angiography provides enough resolution to assess canine coronary arteries.

Introduction

Conventional angiography of the coronary arteries is currently the reference method for the assessment of coronary artery disease in humans and animals, but in veterinary medicine the scientific literature is scant.[1,2,3] This technique is invasive and associated with potential risk of death in humans and, therefore, is recommended in selected clinical conditions, especially in any pathology that can lead to luminal compromise of the coronary arteries.[1,4]

Coronary computed tomography angiography (CCTA) achieved with multidetector computer tomography (MDCT) has been suggested for non-invasive evaluation of the coronary arteries in humans with low to medium risk factors (e.g. aged patients, renal insufficiency, uncontrolled diabetes mellitus and morbid obesity),[5] as an alternative to conventional angiography. The CCTA has been largely facilitated by the use of the electrocardiogram (ECG)-gating technique, which links the acquisition and reconstruction of images to a specific phase in the cardiac cycle, enabling optimal visualization of the entire coronary arteries. The ECG is recorded during scanning, hence all images are synchronized with the cardiac cycle; since the most quiescent part of the heart cycle is the diastolic phase (R-R interval), the most suitable coronary view is obtained during this phase.[6] The use of MDCT-64 slices to assess the coronary tree, in comparison with MDCT-16 slices, has improved the view of smaller arterial branches, allowing reliable non-invasive diagnosis of coronary artery disease in humans.[7]

In dogs, there is still paucity of imaging findings about coronary arteries; knowledge of individual anatomic variations would be important to better understand cardiac vascular abnormalities in this species and, possibly, to prevent complications that might result in death during interventional cardiology procedures, such as diminished coronary blood flow or avulsion of the aberrant coronary artery during pulmonic valve balloon dilation.[3] Three subtypes of branching patterns of the left main coronary artery (LMCA) have been demonstrated in dogs based on corrosion casting techniques,[8] but

they have never been thoroughly classified by CCTA. A recent MDCT-64 slices study carried out in four healthy Beagles described a protocol consisting of the administration a vasodilator and a β-blocker (nitroglycerin and esmolol, respectively) during anesthesia.[9] Furthermore, there is yet a limited number of available MDCT-64 slices and last generation MDCT scanners in the veterinary market, thus it would be important to understand if less performing but more accessible instruments, such as the MDCT-16 slices, provide enough resolution to adequately depict the coronary tree in dogs.

Hence, the aim of this study was to perform an ECG-gated MDCT-16 slices scanner in a large cohort of dogs and verify if the coronary arteries can be adequately visualized, that is, with enough temporal and spatial resolution. In addition, to increase current knowledge on the canine coronary arteries, detailed description of their anatomy based on CCTA findings was provided.

Material and methods

Animals

Dogs scheduled for a CT examination comprehensive of the thoracic region, which was performed to characterize cardiac or extra-cardiac diseases, were included if informed consent to participate in the study was provided by the owner. The study protocol was approved by the ethical committee of the University of Padua, Italy (permission number: 54/2016).

CCTA

All examinations were achieved with a MDCT-16 slices scanner*. After pre-anesthetic assessment, each dog received 0.03 mg/kg of acepromazine†, IM. Thirty minutes later, dogs were gently clipped on the thorax to apply ECG patches, and a 18-20 gauge catheter was placed in the left cephalic vein to inject fluids and medications, if necessary during anesthesia. A second catheter, similar to the former, was placed in the right cephalic vein to administer the contrast medium‡. Thereafter, general anesthesia was induced with a 0.005 mg/kg fentanyl§ bolus, given IV over 3 minutes, followed by propofol IV∞ to effect; dogs were positioned in sternal recumbency and were connected to an anesthetic machine# to control ventilation in order to maintain normocapnia ($EtCO_2$ 40 ± 5 mmHg), and to administer isoflurane∅ for the maintenance of general anesthesia in a fresh gas flow mixture of air and oxygen. All dogs were connected to a multiparameter monitor** to control standard vital parameters. Then, 0.2 mg/kg of atracurium††, was administered IV to achieve transient apnea during the CT scans. If the heart rate went above 100 beats per minute, a 0.0003 mg/kg dexmedetomidine‡‡ bolus, IV, was administered in order to reduce cardiac frequency. Each dog underwent a pre- and a post-contrast CT scan of the region of interest (e.g. total body, thorax, thorax and abdomen, etc) as originally planned by the attending veterinarian, including an ECG-gated scan, set to study the coronary arteries. Iodinated non ionic contrast medium was administered IV at a flow-rate of 3 ml/s through a single-head power

injector system§§ with a total dose of 2 ml/kg, at maximum pressure limits of 300 pound per square inch. Nevertheless, if the exam was only requested for the assessment of possible aberrant coronary arteries, a variable dose of 1-1.5 ml/kg of contrast medium was used (1 ml/kg and 1.5 ml/kg for dogs with body weight >10 kg and ≤10 kg, respectively). The time-to-peak enhancement needed to determine the starting delay of the study was set by using Smart Prep technology feature proprietary§, drawing the region of interest (ROI) within the lumen of the left atrium (Fig. 1). A left atrium opacification threshold of 50 Hounsfield Units (HU) above baseline was used for starting the coronary scan. The starting point of the CCTA scan was set at the level of the main pulmonary trunk and ended at the dome of the diaphragm (including the whole heart) in each dog. The helical retrospective ECG-gated scanning parameters were 80-120 kV (depending on the size of the dog), 300-400 mA, 0.5 s gantry rotation time, 20 mm detector collimation (1.25 mm × 16 slices), heart rate adapted variable pitch (SnapShot Segment-Burst feature proprietary§) with the field of view (FOV) centered on the heart and set as small as possible to include its entire shadow. During the post processing manipulation of data, images were reconstructed with a standard reconstruction kernel in multiple data sets with the temporal reconstruction window of 10% within the cardiac cycle, centered over the 5-95% R-R interval (Fig. 2). Images were reviewed by one board-certified veterinary radiologist (EA) and two board-certified physician radiologists (TK and FA) on a dedicated work station with proprietary software∞∞. Since there is lack of literature describing coronary arteries imaging in dogs, arbitrary criteria were used to classify the CCTA, including:

a) the degree of opacification, which was subjectively defined as poor, moderate, good and excellent;

b) the choice of optimal R-R reconstruction interval for both left coronary artery (LCA) and right coronary artery (RCA);

c) the coronary dominance (right, left or codominance), which was defined by the coronary artery (LCA or RCA) going beyond the *crux cordis*, either directly or through its short or long branches, and

by the origin of the subsinuosus interventricular branch;[10,11]

d) the classification of subtypes of the left main coronary artery (LMCA) branching pattern, as previously described by using a classification system proposed in an anatomical study demonstrated by a corrosion casting technique.[8] In that study, three main subdivisions of the LMCA were noted. In particular, in type 1 LMCA, three major divisions arise from a short common trunk after its origin from the aorta: the *ramus inter-ventricularis paraconalis* (IVP), the *ramus circumflexus* (CX) and the *ramus septi inter-ventricularis* (SI). In type 2 LMCA, the common trunk gives origin to two major branches, CX and IVP, and the LS branch arises directly from the IVP. In type 3 LMCA, no common trunk is present and the CX and IVP originate from the left Valsalva sinus as two distinct vessels; the SI arises from the CX shortly after its origin.[8]

e) the diameter and length of the LCA and RCA and classification of their branches, using a previously described segmental coding system (SCS) whereby the portion of the artery that is located between two reference points is considered to be an angiographic segment.[9,12]

The maximum diameter of the vessel was measured at the origin of each coronary branch and the length of each measurable coronary branch was calculated by using a semi-automated vessel track function$^{\infty\infty}$.

Statistical analysis

The Pearson's chi-squared test was used to identify linear correlations between body weight and diameter or length of the LMCA, left septal coronary artery, left circumflex coronary artery, left interventricular coronary artery and right main coronary artery. The r correlation coefficient, 95% confidence interval and p-values were calculated for each contrast. A Shapiro-Wilk test was performed to assess whether the datasets were normally distributed. Analyses were achieved with commercial software (SPSS v20.0 for Windows). To assess whether the diameter of each coronary artery was

different between dogs with and without pulmonic valve stenosis the Mann-Whitney U test was used. The diameter of coronary arteries was normalized against body weight to account for the size of dogs.

Results

Animals and feasibility of CCTA

Thirty-two dogs were included in the study. The CCTA of the coronary arteries with ECG-gated MDCT-16 slices scanner was successfully performed in 24 dogs (75%) (Fig. 3); eight dogs (25%) were excluded because of an intrathoracic mass altering the normal branching patterns of the coronary arteries (five dogs) or causing cardiac arrhythmia during general anesthesia (three dogs) and leading to poor spatial and contrast resolution. Of the 24 dogs retained in the analysis (signalment and underlying disease reported in Table 1), 12 were male and 12 female, the mean age was 70 ± 37 months and the mean body weight was 26 ± 14 kg. Among breeds, six were crossbreed, two each were, French Bulldog, German Shepherd and Labrador Retriever, and one each was American Bulldog, American Staffordshire Terrier, Cocker Spaniel, English Bulldog, Golden Retriever, Husky, Jack Russel Terrier, Malinois, Spitz, Tibetan Terrier, Weimaraner and Yorkshire Terrier.

No complication associated with the adopted anesthetic protocol was documented during the procedure in any dog. The duration of the CCTA examination was approximately 15 min per dog. The mean heart rate (HR) during the scanning time was 68 ± 20 bpm. The mean time-to-peak left atrial enhancement occurred 11.7 ± 5.5 s after the beginning of contrast medium injection.

CCTA findings

Opacification and R-R reconstruction

Based on the criteria used to evaluate CCTA, the degree of opacification of the coronary arteries was subjectively judged to be excellent in five (21%) dogs and good in the remaining 19 (79%) dogs. The choice of optimal R-R reconstruction interval for both LCA and RCA arteries was 75% in 15 dogs (63%), 70% in five (21%), 80% in two (8%), 65 % in one (4%) and 40% in the remaining case (4%). With regard to coronary dominance, all 24 dogs (100%) showed left dominance.

LMCA branching patterns

Six dogs (25%) of the study matched the type 1 LMCA, nine dogs (37%) the type 2 LMCA and only one (4%) dog the type 3 LMCA.

Four additional branching patterns were noted in the present series and were arbitrarily named type 4, 5, 6 and 7 LMCA. In type 4 LMCA, three major divisions arose from a short common trunk as in type 1 but an additional efferent vessel, arbitrarily named intermediate interventricularis paraconalis branch (IIVP), started from the IVP shortly after its origin, running dorsally and laterally along the lateral wall of the left ventricle. Three dogs (13%) met the type 4 LMCA pattern. In type 5 LMCA, no common trunk was present and the CX and IVP originate distinctly as in type 3 but the SI arose from the IVP. Three dogs (13%) of our case series matched the type 5 LMCA. In type 6 LMCA the IVP, the CX and SI originated from the short common trunk; an additional SI arose from the IVP. This type was found in one dog (4%). Lastly, in type 7 LMCA the CX and IVP originated from a common trunk but no septal branch was visible. This type was found in one dog (4%). No aberrant right or left coronary arteries were found in any of the 24 dogs. An illustrative drawing of LMCA classification is provided (Table 2). Of note, in the dog with type 3 LMCA an intra-myocardial bridging (tunneling) of the proximal third of the IVP was noted; more specifically, this portion of the IVP was running 6 mm deep within the myocardium for a short path, emerging downstream into the pericardial fat (Fig. 4).

Segmentation of the coronary arteries

Ramus circumflexus

Both left and right coronary arterial branches were further classified, by adapting a previously described SCS.[9,12] The LCA originated from the left sinus of Valsalva in all 24 dogs (100%). When the LMCA was present, it was classified as a single distinct segment (LMCA1) before branching off, as

above classified; the CX and IVP were divided in three segments (Fig. 5 and 6), the SI in two segments and the RCA in three segments (total of 12 angiographic segments). The three segments of the CX were named: CX1 (cranial segment), CX2 (lateral segment) and CX3 (caudal segment). The CX1 runs caudally and ventrally to the left auricle; a variable number (1-4) of efferent vessels were branching off at this level and running caudo-laterally along the lateral surface of the myocardium of the left ventricle. The CX1 segment ends at the level of the first branching off vessel, arbitrarily named marginal CX1. The CX2 runs perpendicular to the scan plane into the coronary groove, laterally to the left atrio-ventricular junction, ventral to the left circumflex vein. The CX3 runs caudo-medially to the left atrium, parallel to the scan plane, along the caudo-dorsal surface of the left ventricle; a variable number of vessels (1-4) were seen branching off at this level and running towards the apex of the heart, arbitrarily named caudal lateral CX3 branches. The CX3 segment continued running in the subsinuosus interventricular groove, ending as the subsinuosus interventricular branch. In one of the 24 dogs a single caudal CX3 branch was seen running along the diaphragmatic surface of the right ventricle.

Ramus inter-ventricularis paraconalis

The IVP artery was classified in three segments: dorsal (IVP1), medium (IVP2) and apical (IVP3). The IVP1 ran along the mid-dorsal aspect of the heart, caudo-ventro-laterally to the left, just caudal to the main pulmonary artery and ventro-medially to the left auricle, almost parallel to the scan plane. The IVP2 continued running caudally along the mid-surface of the heart, within the paraconal interventricular groove before ending as IVP3 along the ventral portion of the heart (apical portion). In three dogs of our case series an additional intermediate branch was originating between the IVP1 and IVP2 segments (type 4 LMCA). In another dog, a small branch was originating from the terminal portion of the IVP1 and running cranially and laterally to the right, supplying the wall of the main pulmonary artery, namely branch pulmonary conus artery.

Ramus septi interventricularis

The septal branch was seen in all except one dog (type 7 LMCA) of our study and ran laterally to the aortic bulb towards the interventricular septum (SI1) and turned perpendicular to the scan plane just ventral to the aortic bulb, supplying the mid-caudal aspect of the interventricular septum (SI2).

Right coronary artery

The RCA was seen in all dogs of our case series, originating from the right sinus of Valsalva and classified in three segments (RCA1, RCA2, RCA3). The RCA1 ran ventrally in the coronary groove, between the main pulmonary trunk and right atrium, almost parallel to the scan plane. The RCA2 turned perpendicular to the scan plane ventro-lateral to the right atrium, into the right atrio-ventricular groove. Between the RCA1 and RCA2 segments a variable number (1-3) of efferent vessels supplying the lateral wall of the right ventricle were detected, arbitrarily named RCA acute marginal branches. The RCA3 ran caudo-dorsally, almost perpendicular to the scan plane, continuing into the right atrio-ventricular groove on the diaphragmatic surface of the heart.

Comparison between coronary arteries

The mean diameter and length of the left and right main coronary arteries are listed in Table 3; correlation coefficients, 95% confidence interval and p-values of body weight with diameter or length of the left and right coronary arteries are also provided. Several significant positive correlations were documented between coronary arteries and body weight, including the diameter of all left and right coronary arteries as well as the length of the left circumflex and interventricular coronary arteries. Of note, the diameter of each coronary artery did not differ between the five dogs (21%) with pulmonic valve stenosis and 19 dogs (79%) without pulmonic valve stenosis.

Discussion

High temporal and spatial resolutions are prerequisites to correctly identifying the coronary arteries.[13] Comparison of coronary angiographic findings between MDCT scanners demonstrated that the 64-slices provides improved image quality and overall visibility of small branches as compared to 16-slices machines in humans.[7] However, it is important to emphasize that the number of slices per se is not the only parameter that influences quality of images during the assessment of coronary arteries.[13] Indeed, also the x-ray tube output and rotation speed, slice collimation, FOV, pitch, type of acquisition (prospective versus retrospective), reconstruction algorithm, heart rate and contrast medium delivery are all parameters that affect image quality. In the present investigation CCTA examination with an ECG-gated MDCT-16 slices scanner provided enough temporal and spatial resolution to assess the coronary tree in 24 dogs. In humans, the target heart rate for optimal CCTA studies is 60-65 bpm.[9] In our dogs the mean heart rate was approximately 70 ± 20 bpm, which is slightly higher than the ideal frequency for humans but lower than previously reported in a study performed in 4 Beagles where the mean heart rate was 110.[9]

The starting delay of the scan was set by using Smart Prep technology feature proprietary§, drawing the ROI within the lumen of the left atrium (Fig. 1). We deemed this ROI location very convenient to study the coronary arteries of dogs during their maximal opacification. In our opinion, setting the ROI in the ascending or descending aorta might lead to a less predictable starting delay, essential to achieve high quality images.

Motion can lead to blurring of the contours of the coronary vessels;[13] in order to decrease this artifact, the choice of the optimal R-R interval is essential during retrospective CCTA ECG-gated acquisition. In our study, both LCA and RCA were optimally evaluated in the 70-75% of the R-R interval; this result slightly differs from that in Beagles where the majority of the coronary segments were more accurately detected in the 75-95% of the R-R interval.[9] This discrepancy might be due to the fact that

our series did not include dogs of Beagle breed but a varied study population and, moreover, a different anesthetic protocol was used. Nevertheless, in line with the previous investigation,[9] coronary arteries of dogs were best visualized during the late-end diastolic phase, where the coronary flow is expected to be maximal and there is less cardiac motion.

Similar to former observations, the heart of dogs showed left coronary dominance,[8,10,11,14] meaning that the majority of the myocardium is perfused by the LCA and its branches. This data does not reflect the myocardial perfusion of humans, being mostly right dominant.[11] Therefore, researchers performing experimental studies in dogs should be aware that the coronary arteries in this species follow a different pattern of distribution.[10]

Some variations of the LMCA branching pattern have been previously described in dogs.[8,9] As reported in one investigation,[8] the most common anatomical variation also observed in the present dogs was the type 2 LMCA. Additionally, we described 4 other types of LMCA branching pattern, which had never been documented with CCTA. Knowledge of the normal coronary anatomy is essential and branching pattern variations should not be mistaken for aberrant coronary arteries. Moreover, CCTA ECG-gated is a complementary diagnostic method that may provide additional information, not only regarding the anatomy of coronary arteries but also concurrent cardiovascular anomalies.[15]

The data regarding the diameter and length of the coronary arteries and their main branches is in agreement with the existing literature,[9,16] supporting the notion that CCTA ECG-gated provides reliable measurement of both LCA and RCA in dogs. As expected, we found positive correlations between body weight and diameter of LCA and RCA and between body weight and length of the CX and IVP, indicating that heavier dogs have bigger coronary arteries. Differently, no correlation was observed between the length of the RCA, LMCA and SI, possibly secondary to the small size and lack of filling of the distal portion of these vessels, leading to their underestimation by CCTA.

Because in the present study five dogs affected by pulmonic stenosis were included, it was verified

whether the diameter of their coronary arteries differed; differences between dogs with pulmonic stenosis and the other cases were not documented, possibly due to the small number of animals in the former group. Hence, further studies are required to confirm this observation.

As commented by previous authors, the ability to depict the normal coronary arteries using CCTA is necessary for characterizing the anatomic variants of dogs.[9] If coronary artery anomalies are present, it is mandatory to understand which branch and which portion of the vessels are involved. For this reason, in humans a standard SCS of the coronary arteries has been proposed.[12] In our series 12 coronary segments were identified by adapting a previously described SCS;[9,12] we believe that when more CCTA studies of coronary anomalies will be available, the comprehensive SCS will be helpful for correctly describing the location and extent of most abnormalities of coronary arteries.

As described in some anatomic articles in dogs,[10,17] an intra-myocardic bridging of the proximal third of the IVP was shown in one of our cases; the epicardial portion of the coronary artery was involved, tunneling below a section of the myocardium. To the best of our knowledge, this is the first case of myocardial bridging described by CCTA in a dog. The clinical significance of this anomaly is uncertain as the majority of coronary arterial flow occurs in diastole, while constriction of the coronary artery by a myocardial bridge is predominately a systolic event.[10] Considering the high prevalence of myocardial bridging described at necropsy in dogs (up to 30%),[17] further studies are clearly needed to understand if this anomaly is associated with impaired myocardial perfusion or any other cardiac sign.

Of note, no evidence of atheromathous coronary plaques was detected in this study. Atherosclerosis, defined as arterial wall thickening due to lipid deposition, is rare in dogs and primarily associated with hypothyroidism, diabetes mellitus, hypertension and hyperthyroidism.[18,19] None of the dogs was suspected to have any of the listed diseases, likely explaining the absence of coronary atherosclerosis in this series.

The main limitation of the study is that the cohort of the dogs included also animals with a congenital

cardiovascular disease, even if in none was the anatomic distribution of coronary arteries affected. In conclusion, the ECG-gated MDCT-16 slices scanner provided enough temporal and spatial resolution to assess coronary arteries in dogs. CCTA should be considered as an alternative imaging technique to conventional coronary angiography, if coronary arteries need to be characterized in dogs.

Footnotes

* 16 –MDCT Lightspeed General Electric Medical System, Bergamo, Italy

† Prequillan, Fatro SpA, Italy

‡ Omnipaque 350 mgI/ml; Iohexol, Titolare AIC, GE healthcare S.r.l., Milan, Italy

§ Fentadon, Dechra Veterinary Products Srl, Italy

∞ Proposure, Merial Italia SpA, Italy

Mindray Ex-Wato 55, Mindray Medical Italy Srl, Italy

∅ Isoflurane Vet, Merial Italia SpA, Italy

** Mindray Beneview T5, Mindray Medical Italy Srl, Italy

†† Acurmil, Lisapharma SpA, Italy

‡‡ Dexdomitor, Orion Pharma, Finland

§§ Medrad envision CT injector, Medrad Italia, Cava Manara, Italy

∞∞ GE healthcare volume share 4.7

Tables

Table 1

	Breed	Gender	Age (months)	Disease
1	Cross-Breed	MC	64	Pericardial effusion
2	Cross-Breed	M	96	Cervical subcutaneous lipoma
3	Labrador	FS	153	Splenic mass
4	Labrador	FS	84	Peripheral vestibular syndrome
5	Cross-Breed	FS	84	Gastrointestinal stroma tumor
6	German Shepherd	F	120	Multicentric lymphoma
7	Cross-Breed	F	96	Thoracolumbar disc herniation
8	Bouledogue Français	FS	48	No disease (referred for suspected mediastinal mass)
9	English Bulldog	M	65	Pulmonic stenosis
10	Spitz	M	24	Pulmonic stenosis
11	German Shepherd	F	120	Peripheral neuropathy
12	Siberian Husky	M	96	Pulmonary thromboembolism
13	Bouledogue Français	FS	84	Heart base tumor
14	Malinois	F	72	Pericarditis
15	Weimaraner	M	80	Cervical spondylomyelopathy
16	American Bulldog	M	74	Lymphoma
17	Golden retrivier	M	80	Pericardial effusion
18	American Staffordshire terrier	M	5	Pulmonic stenosis
19	Yorkshire Terrier	M	120	Heart base tumor
20	Cocker Spaniel	F	4	Persistent right fourth aortic arch
21	Jack Russel Terrier	M	27	Pulmonic stenosis

22	Cross-Breed	M	86	Pulmonic stenosis
23	Cross-Breed	F	100	Heart base tumor
24	Tibetan Terrier	F	80	Tetralogy of Fallot
25	Labrador	FS	70	Right auricle cardiac tumor
26	Labrador	M	72	Multiple vascular anomalies
27	Dogue de bordeaux	M	84	Heart base tumor
28	Pitt Bull	M	12	Cor triatriatum dexter
29	Golden Retriver	M	60	Mesothelioma
30	Cross-Breed	M	80	Heart base tumor
31	Cross-Breed	F	100	Heart base tumor
32	German Shepherd	M	153	Heart base tumor

F = female; M = male; FS= female spayed; MC= male neutered.

Table 2. An illustrative drawing of all types of LMCA classification ((1) LMCA, (2) *ramus circumflexus*, (3) *ramus inter-ventricularis paraconalis*, *(4) ramus septi inter-ventricularis*, (5) RCA, (6) intermediate *inter-ventricularis paraconalis* branch, (7) additional *ramus septi inter-ventricularis*.

LMCA classification	**% of dogs**	**Illustrative drawing**
Type 1	25%	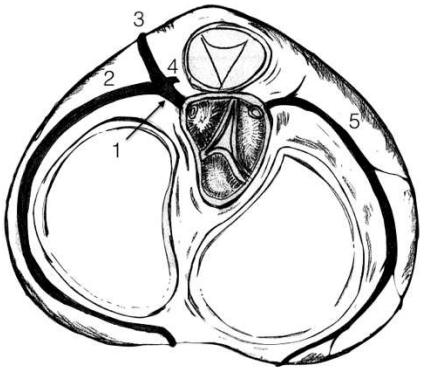
Type 2	37%	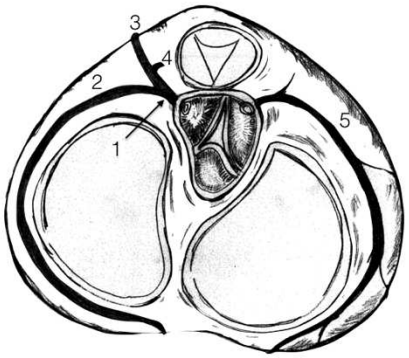
Type 3	4%	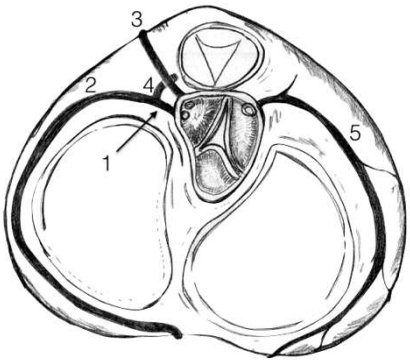

Type 4	13%	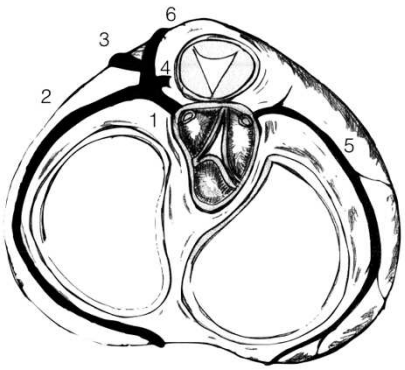
Type 5	13%	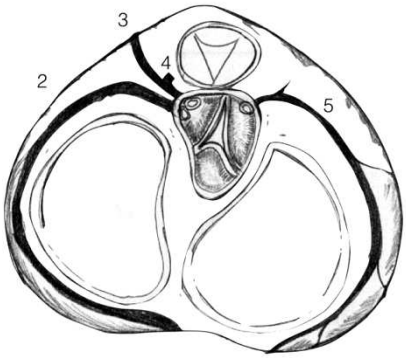
Type 6	4%	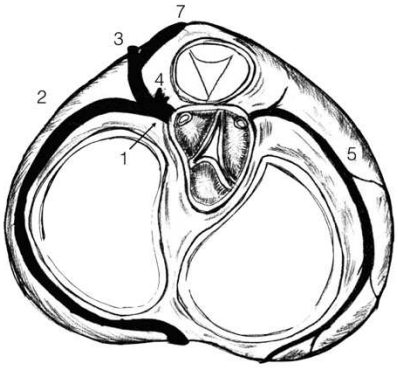
Type 7	4%	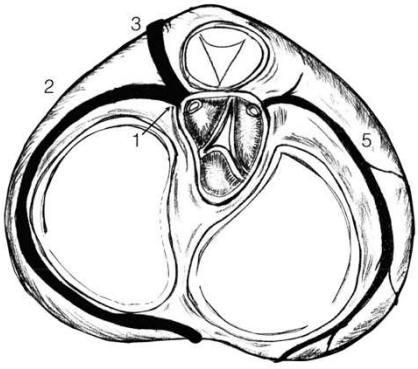

Table 3. Correlation between body weight and diameter or length of the left and right coronary arteries.

Body weight vs. left coronary arteries:				
	mean±sd of coronary arteries (mm)	coefficient r	95% confidence interval	p-value
LMCA				
diameter	4.0±1.3	0.630	0.230 to 0.847	0.005
length	3.6±1.0	0.327	-0.135 to 0.672	0.159
Septal				
diameter	1.6±0.5	0.651	0.316 to 0.842	0.001
length	34.3±12.4	0.445	0.003 to 0.742	0.051
Circumflex				
diameter	2.9±1.0	0.840	0.654 to 0.930	<0.001
length	76.9±22.2	0.865	0.691 to 0.944	<0.001
Interventricular				
diameter	2.5±0.8	0.870	0.714 to 0.944	<0.001
length	76.7±27.1	0.765	0.498 to 0.900	<0.001
Body weight vs. left coronary arteries:				
	mean±sd of coronary arteries (mm)	coefficient r	95% confidence interval	p-value

RCA				
diameter	2.0±0.5	0.667	0.351 to 0.847	<0.001
length	78.7±66.1	-0.125	-0.528 to 0.325	0.591

All datasets were normally distributed.

Figure captions

Figure 1. Region of interest (ROI) drawn within the lumen of the left atrium to standardize the starting delay time of the CCTA study by using Smart Prep technology feature proprietary.

Figure 2. Reconstruction interval of the ECG gating expressed as percentages of the R-R interval.

Figure 3. Volume rendering of the heart and coronary tree.

Figure 4. Intra-myocardial bridging (tunneling) of the proximal third of the IVP displayed as curved MPR reconstruction.

Figure 5. CX branches classified, by adapting a previously described SCS, displayed as curved MRP reconstruction.

Figure 6. IVP branches classified, by adapting a previously described SCS, displayed as curved MRP reconstruction.

References

1. Nieman K., Oudkerk M., Rensisn B.J., van Ooijen P., Munne A., van Geuns RJ, de Feyter PJ. (2001) Coronary angiography with multi-slice computed tomography, Lancet. 357, 599-603.
2. Napp A.E., Hasse R., Laule M., Schuetz G.M., Rief M., Dreger H., Feuchtner G., Friedrich G., Spacek M., Suchanek M., Kofoed K.F. & Engstroem T. (2017) Computed tomography versus invasive coronary angiography: design and methods of the pragmatic randomised multicentre DISCHARGE trial, Europea Radiology. 27, 2957-2968.
3. Fonfara S, Martinez Pereira Y, Swift S, Copeland H, Lopez-Alvarez J, Summerfield N, Cripps P, Dukes-McEwan J. (2010) Balloon valvuloplasty for treatment of pulmonic stenosis in English Bulldogs with an aberrant coronary artery. J Vet Intern Med. 24, 354-9.
4. Karl Poon and Darren Walters (2011). Indications for Coronary Angiography, Advances in the Diagnosis of Coronary Atherosclerosis, Prof. Suna Kirac (Ed.), InTech, DOI: 10.5772/19106. Available from: https://www.intechopen.com/books/advances-in-the-diagnosis-of-coronary-atherosclerosis/indications-for-coronary-angiography
5. Morteza Tavakol MD, Salman Ashraf MD, Sorin J Brener MD. (2012) Risks and complications of coronary angiography comprehensive review, Global Journal of Health Science. 4, 65-93.
6. Mahesh M, Cody DD. (2007) Physics of cardiac imaging with multiple-row detector CT. Radiographics. 27, 1495-509. Review.
7. Wang YN, Jin ZY, Kong LY, Zhang ZH, Song L, Zhang SY, Zhang LR, Lin SB, Wang Y, Zhao WM. (2006) Comparison of coronary angiography between 64-slice and 16-slice spiral CT. Zhongguo Yi Xue Ke Xue Yuan Xue Bao. 28, 26–31.
8. Noestelthaller A1, Probst A, König HE. (2007) Branching patterns of the left main coronary artery in the dog demonstrated by the use of corrosion casting technique. Anat Histol Embryol.

36, 33-7.

9. Drees R., Frydrychowicz A., Reeder S.B., Pinkerton M.E., Johson R. (2001), 64-Multidetector Computed Tomographic Angiography of the canine coronary arteries , Veterinary Radiology & Ultrasound. 52, 507–515.
10. Scansen B.A. (2017) Coronary Artery Anomalies in Animals. Vet. Sci. 4, 20; doi:2.3390/vetsci4020020
11. De Oliveia C.L.S., David G.S., Carvalho M., Dornelas D., Araùjo S., Da Silva N.C., Ruiz C.R., Fernandes J.R., Wafae N. (2011) Anatomical Indicators of Dominance between the Coronary Arteries of Dogs. Int. J. Morphol. 29, 845-849.
12. Austen WG, Edwards JE, rye RL, Gensini GG, Gott VL, Griffith LS, McGoon DC, Murphy ML, Roe BB, (1975) A reporting system on patients evaluated for coronary artery disease. Report of the Ad Hoc Committee for Coronary Artery Disease, Council on Cardiovascular Surgery, American Heart Association. Circulation. 51, 5-40.
13. Achenbach S. (2006) Computed tomography coronary angiography. J Am Coll Cardiol. 21, 1919-28.
14. Emil Blair, (1961), Anatomy of the ventricular coronary arteries in the dog. Circulation research. 9, 333-341
15. Laborda-Vidal P, Pedro B, Baker M, Gelzer AR, Dukes-McEwan J, Maddox TW. (2016) Use of ECG-gated computed tomography, echocardiography and selective angiography in five dogs with pulmonic stenosis and one dog with pulmonic stenosis and aberrant coronary arteries. J Vet Cardiol. 18, 418-426.
16. Evans HE. (1993) The heart and the arteries. In: Evans HE (ed): Miller's anatomy of the dog. Philadelphia: Saunders, 598-601

17. Tangkawattana P, Muto M, Nakayama T, Karkoura A, Yamano S, Yamaguchi M. (1997) Prevalence, vasculature, and innervation of myocardial bridges in dogs. Am J Vet Res. 58, 1209-15.
18. Boynosky NA, Stokking L. (2014) Atherosclerosis associated with vasculopathic lesions in a golden retriever with hypercholesterolemia. Can Vet J. 55, 484-8.
19. Hess RS, Kass PH, Van Winkle TJ. (2003) Association between diabetes mellitus hypothyroidism or hyperadrenocorticism and atherosclerosis in dogs. J Vet Intern Med, 17, 489-94.